



## Fe (III) removal by activated carbon produced from Egyptian rice straw by chemical activation

M.E. Ossman<sup>a,b,\*</sup>, M. Abdel Fatah<sup>a</sup>, Nahla A. Taha<sup>b</sup>

<sup>a</sup>Faculty of Engineering, Petrochemical Engineering Department, Pharos University, Alexandria, Egypt  
Tel. +20 100 1392281; email: mhr1410@hotmail.com

<sup>b</sup>City for Scientific Research and Technological Application (CSAT), Alexandria, Egypt

Received 24 December 2012; Accepted 9 April 2013

---

### ABSTRACT

The present work explored the use of Egyptian rice straw, an agricultural waste that leads to global warming problem through brown cloud, as a potential feedstock for the preparation of activated carbon. Chemical activation of this precursor using two different methods was adopted. The produced activated carbon was fully characterized considering its adsorption properties, as well as its chemical structure and morphology. Application of using the produced activated carbon and raw rice straw for removal of the Fe(III) was evaluated in a batch operation system. The results indicated that the rate of uptake of the Fe(III) is rapid in the beginning and 80% adsorption is completed within 50 min, and the time required for equilibrium adsorption is 60 min. The removal efficiency of Fe(III) depends on the pH of the solution. The optimal Fe(III) removal efficiency occurs at pH 5. The adsorption isotherm analysis showed that the Freundlich isotherm provides a good model for the sorption system. The  $1/n$  is lower than 1.0, indicating that Fe(III) is favorably adsorbed by activated carbon.

*Keywords:* Chemical activation; Rice straw; Fe(III); Adsorption; Activated carbon

---

### 1. Introduction

Activated carbons are carbonaceous materials that can be distinguished from elemental carbon by the oxidation of the carbon atoms found on the outer and inner surfaces [1]. These materials are characterized by their extraordinary large specific surface areas, well-developed porosity, and tunable surface-containing functional groups [2]. For these reasons, activated carbons are widely used as adsorbents for the removal of organic chemicals and metal ions of environmental or economic concern from air, gases, potable water,

and wastewater [3]. Activated carbon can be synthesized by two methods: chemical and physical activation. In chemical activation, the starting materials (raw material) are impregnated with a strong dehydrating agent, followed by pyrolysis at high temperature to prepare activated carbon. Physical activation method consists of carbonization of the precursor (raw) material in an inert atmosphere and gasification of the resulting char in the presence of steam, carbon dioxide, or air. Activated carbon can be prepared from many organic materials having high carbon content, like coal [4], wood [5,6], lignite [7], coconut shells [8,9], and activated sludge [10]; and recently, many

---

\*Corresponding author.

agricultural byproducts, such as walnut shells [11], palm shells [12], pecan shells [13,14], date stones [15], almond shells [16], sugar cane bagasse [17], cotton stalks, [18] Physic nut [19], and rice straw [20,21], have been used as sources for activated carbon production. The aim of this work is to produce activated carbon from Egyptian rice straw by chemical activation, study the characterization of the produced activated carbon, and then use the produced activated carbon as adsorbent for the removal of Fe(III) from waste water, and study the variables affecting the removal process, such as initial concentration, pH, and weight of adsorbent. Additionally, the kinetic and thermodynamic properties were determined to interpret and elucidate how the adsorption mechanism of Fe(III) ions works. The kinetics studies showed that the adsorption of Fe(III) on activated carbon followed the pseudo-second-order model.

## 2. Materials and methods

### 2.1. Materials

Rice straw used as the adsorbent in this study was collected from a cultivated area near Behira City. The straw was washed with distilled water several times and dried at room temperature. The straw was dried in a drying furnace at 150°C for two hrs, ground and sieved between 400 and 600 µm, and stored in a plastic bottle prior to use. All chemicals were of analytical grade reagent and the glassware were Pyrex washed with soap, rinsed thoroughly, and then washed with deionized water.

### 2.2. Preparation of activated carbon from rice straw

The preparation of activated carbon by activation process takes place by two different methods. The activation procedure to produce AC1 was carried out in a 2 L beaker where a sample of 200 g of dried rice husks was mixed thoroughly with 200 mL of concentrated sulfuric acid. The mixture was heated to 200°C with continuous agitation for 1 h. During activation, water was evaporated and the mixture became slurry and started to solidify. At this moment, agitation was stopped while heating continued until the produced material became a carbon-like material. A trace amount of distilled water was injected into the carbonized material using 10 mL syringe to promote activation. Then, the resulting carbon was allowed to cool to room temperature, washed with distilled water, soaked in dilute potassium hydroxide solution for 30 min, washed a second time with distilled water, dried, and stored in a closed container for

characterization. The activation procedure to produce AC2 is as follows: the carbonization of the dried rice husks was carried out using a muffle furnace which allows limited supply of air. Carbonization was done at 350°C for two hours and allowed to cool to room temperature for three hours before activation. Then, a carefully weighed  $25.0 \pm 0.01$  g carbonized carbon was placed in a beaker containing 500 cm<sup>3</sup> of potassium permanganate (KMnO<sub>4</sub>). The content of the beaker was thoroughly mixed and heated until it formed a paste. The paste was then transferred to an evaporating dish which was placed in a furnace and heated at 300°C for 30 minutes. This was allowed to cool and washed with distilled water to a pH of  $6.7 \pm 0.12$ , oven-dried at 105°C for one hour to a constant weight, and ground. A fine powdered fluted activated carbon, which was kept in an airtight vial, was used for the various experiments.

### 2.3. Characterization of activated carbon

#### 2.3.1. Iodine number

The iodine number (mg/g of activated carbon) was evaluated using the procedure proposed by the standard test method (ASTM D 4,607–86). The activated carbon (approximately 0.3–0.6 g) was placed in a 250 mL dry Erlenmeyer flask and was fully wetted with 10 mL HCl 5%. Then, 100 mL of iodine solution (0.1 M) was poured into the flask and the mixture was vigorously shaken for 30 s. After a quick filtration, 50 mL of the solution was titrated with sodium thiosulfate (0.1 M) until the solution became pale yellow. Two milliliters of starch indicator solution (1 g/L) was added and the titration was continued with sodium thiosulfate until the solution became colorless. The concentration of iodine in the solution was, thus, calculated from the total volume of the sodium thiosulfate used.

#### 2.3.2. Morphology analysis

In order to know the structure sight of the activated carbon, scanning electron microscopy (SEM) was employed to visualize sample morphology. In the present work, the activated carbon prepared was analyzed by this technique using SEM "JEOL JSM 6360LA" to study the surface morphology of the activated carbon and qualitative elemental analysis.

#### 2.3.3. IR spectroscopy analysis

The surface functional groups and structure were studied by FTIR spectroscopy. The FTIR spectra of the raw material and the resulting activated carbon were

recorded between 500 and 4,000  $\text{cm}^{-1}$  in FTIR- 8,400 S Shimadzu.

#### 2.2.4. Batch studies

Single-stage batch adsorption tests were conducted on 200 mL Fe(III) solutions contained in flasks by stirring, using a IKA RT5 model magnetic stirrer operated at 200 rpm. Samples with various Fe(III) concentrations were prepared from the stock solution to get various values of final equilibrium concentrations of Fe(III) (30–150 ppm). The amount of solute adsorbed per unit gram of adsorbent  $q_e$  (mg/g) was evaluated from the equation:

$$q_e = \frac{v(C_0 - C_e)}{M} \quad (1)$$

where  $V$  is the volume of the solution,  $C_0$  is the initial concentration of the adsorbate solution,  $C_e$  is the concentration of the solute in the bulk phase at equilibrium, and  $M$  is the mass of the adsorbent.

### 3. Results and discussion

#### 3.1. Characterization of the produced carbon

##### 3.1.1. Physico-chemical properties of the activated carbon

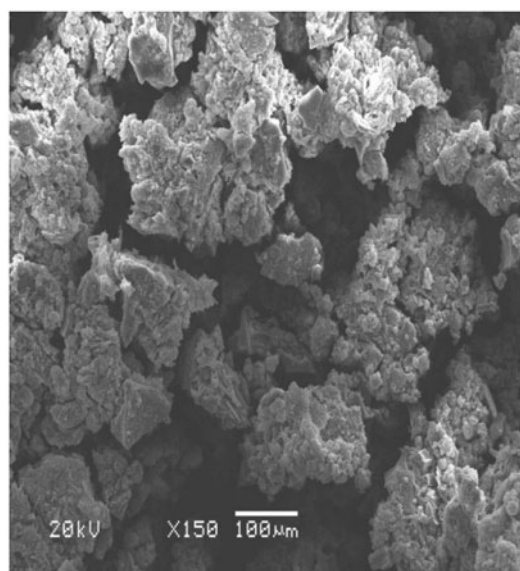
Some properties of the activated carbon are presented in Table 1. The activated carbon product has iodine a value about 815 mg/g and a porous volume equal to 0.0731  $\text{cm}^3/\text{g}$ . The AC is composed mainly of carbon, but also has lots of oxygen from many oxygenated surface functions. We also note the presence (15% compared to the carbon content) of potassium in AC1 due to treatment with potassium hydroxide during the activation step.

Table 1  
Physico-chemical properties of the activated carbon

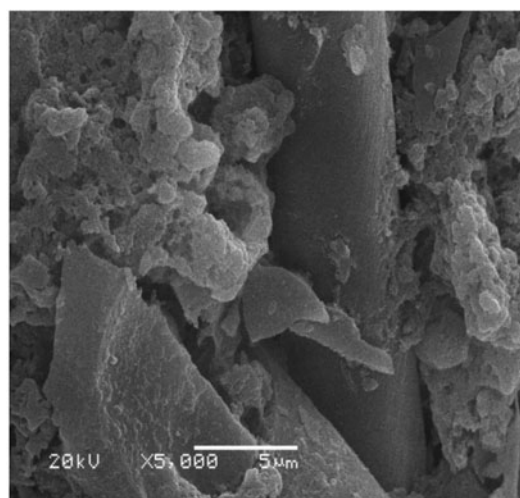
Parameter	Value	
	AC1	AC2
Specific surface area ( $\text{m}^2/\text{g}$ )	962.5	956.52
Porous volume ( $\text{cm}^3/\text{g}$ )	0.312	0.791
Carbon (%)	52.49	49.41
Oxygen (%)	31.3	34.13
Potassium (%)	0.432	8.977
Si (%)	1.739	1.321
Ash content (%)	4.8	2
Iodine number (mg/g)	815.525	735.24

#### 3.1.2. Surface morphology

SEM images with different levels of magnification factor are taken for treated rice straw in order to show the major features of the fibers' morphology after treatment. Figs. 1 and 2 show the SEM images for activated carbon produced from rice straw (AC1) and (AC2) with magnification factor 150 and 250, respectively, which aid in investigating the total surface of treated fibers as flocculated particles. By increasing the magnification factor (from 150 to 5,000) as in Figs. 1 and 2, it is obvious that the high

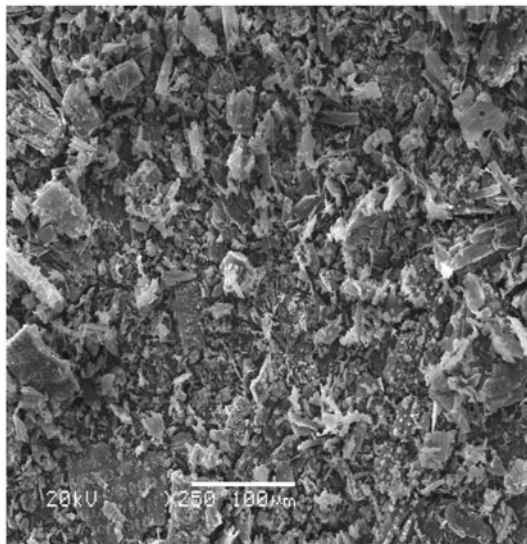


(a)

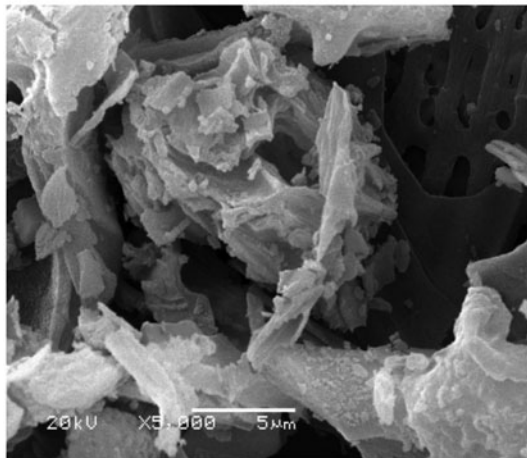


(b)

Fig. 1. (a) SEM for activated carbon produced from rice straw (AC1) with magnification factor 150, (b) magnification factor 5,000.



(a)



(b)

Fig. 2. (a) SEM for activated carbon produced from rice straw (AC2) with magnification factor 250, (b) magnification factor 5,000.

surface roughness increases the surface area of adsorption.

### 3.1.3. FTIR for collected figure (comparison between the three types of treatment of rice straw)

The FTIR analysis permits spectrophotometric observation of treated rice straw in the range  $400\text{--}4,000\text{ cm}^{-1}$  and serves as a direct means for the identification of the organic function on the surface. An examination of the treated rice straw provides information regarding the surface groups that might have participated in the adsorption reaction and also indicates the surface site (s) on which adsorption can take

place. In Fig. 3 IR studies indicate the participation of the specific functional groups in adsorption interaction. The IR spectrum of the treated rice straw (Fig. 4) showed that the most prominent peaks in the spectrum originate from OH vibrations ( $3,300\text{--}3,450\text{ cm}^{-1}$ ) and C–H asymmetric and symmetric stretching vibrations at ( $2,935\text{--}2,300\text{ cm}^{-1}$ ). Very intense peaks in the region ( $1,550\text{--}1,640\text{ cm}^{-1}$ ) originate from the stretching mode of N–H group, at ( $700\text{--}1,300\text{ cm}^{-1}$ ) stretching may be due to the of C–C group, and at ( $400\text{--}700\text{ cm}^{-1}$ ) stretching may be due to the aromatic region related to C–O group.

### 3.2. Effect of contact time

In order to establish the equilibration time for maximum uptake and to know the kinetics of the adsorption process, the adsorption of Fe(III) on activated carbon produced from rice straw by chemical activation (AC1 and AC2) and raw rice husk (Raw) as adsorbents was

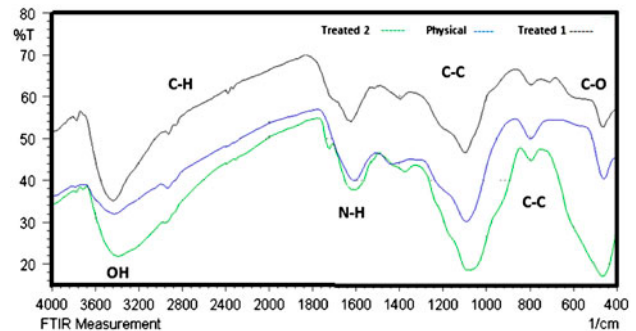


Fig. 3. FTIR for activated carbon produced from rice straw.

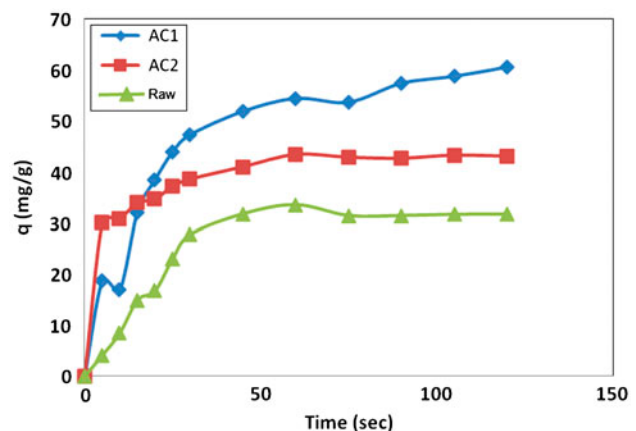


Fig. 4. The effect of contact time on the adsorption capacity for AC1, AC2, and Raw. Conc. of Fe (III) is 30 ppm, pH is 5, weight of adsorbent is 2 g/l, and Temperature is  $25\text{ }^{\circ}\text{C}$ .

studied as a function of contact time and results are shown in Fig. 4. It is seen that the rate of uptake of the Fe(III) is rapid in the beginning and 80% adsorption is completed within 50 min. Fig. 4 also indicates that the time required for equilibrium adsorption is 60 min., and it is found that AC1 has higher adsorption capacity than AC2 and raw rice husk.

The effect of concentration on the equilibration time was also investigated as a function of initial Fe(III) concentration and the results are shown in Fig. 5. It was found that time of equilibrium, as well as time, required to achieve a definite fraction of equilibrium adsorption which is independent of initial concentration.

### 3.3. Effect of pH

The effect of pH on the equilibrium uptake of Fe(III) was investigated by employing the initial concentration of Fe(III) ( $30\text{mgL}^{-1}$ ) and  $1\text{gL}^{-1}$  of adsorbent. The initial pH values were adjusted with 0.1M HCl or 0.1M NaOH to form a series of pH from 3 to 9. The suspensions were shaken at room temperature ( $25 \pm 2^\circ\text{C}$ ) using agitation speed (200 rpm) for the equilibrium time (60 min) and the results are represented in Fig. 6.

It can be observed that the removal efficiency increases with increasing initial pH and it almost reaches a peak value around 5, and then decreases with increasing initial pH. Then, the optimal Fe (III) removal efficiency occurs at pH 5. This result is considerably consistent with eggshells, olive cake, and chitin adsorbents [22–24].

The results can be explained as follows: at low pH, the concentration of proton is high, so iron ions' binding sites become positively charged and then metal cations and protons compete for binding sites of

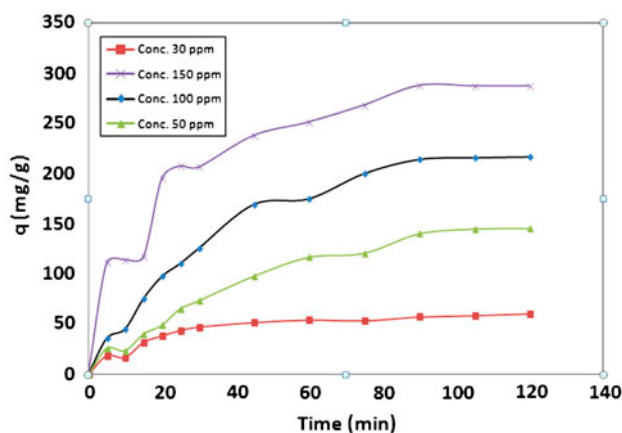


Fig. 5. The effect of contact time on the adsorption capacity for AC1 at different concentration of Fe(III). pH is 5, weight of adsorbent is 2 g/l, and Temperature is  $25^\circ\text{C}$ .

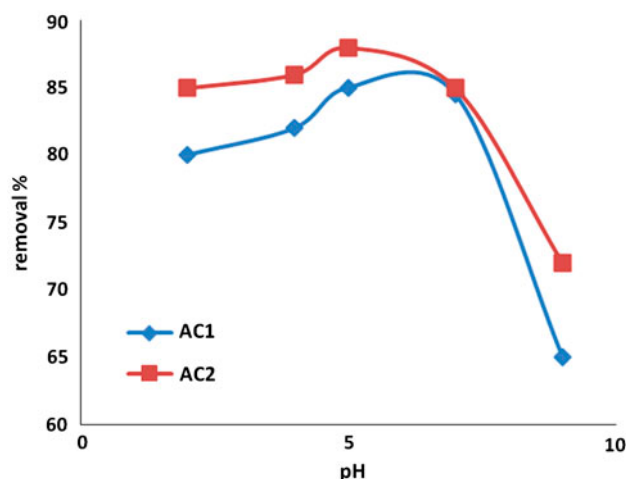


Fig. 6. Effect of initial pH on the removal efficiency % of Fe (III) ions. (initial concentration of Fe(III): 30 ppm, weight of adsorbent: 1 g /l, Contact time: 1 h).

activated carbon which results in lower uptake of iron ions. As pH increases in ranges from 3 to 5, the concentration of proton existing in the solution will be decreased, and hence will not give the chance to compete with iron ions on the adsorption sites of activated carbon, thus facilitating greater Fe(III) ions uptake. After pH 5, the removal efficiency decreases as pH increases, which is due to the precipitation of insoluble iron hydroxide in the solution. Therefore, at these pH values, both the adsorption and precipitation are effective mechanisms to remove the iron (III) in aqueous solution. The iron cations in aqueous solution convert to different hydrolysis products [25].

### 3.4. Effect of weight of adsorbent

The results of the experiments with varying adsorbent dosage are presented in Fig. 7. It was found that with an increase in the adsorbent dosage from 0.2 to 5.0 g/L, the removal of Fe(III) increases from 60 to 90% in case of AC1. This can be explained by the fact that more the mass available, more the contact surface offered to the adsorption. These results are qualitatively in good agreement with those found in the literature [24].

### 3.5. Equilibrium of adsorption

Adsorption isotherms are used to determine the capacity and optimize the use of the adsorbent at equilibrium. Therefore, the correlation of equilibrium data by either theoretical or empirical equations is essential to the practical design and operation of the adsorption systems.

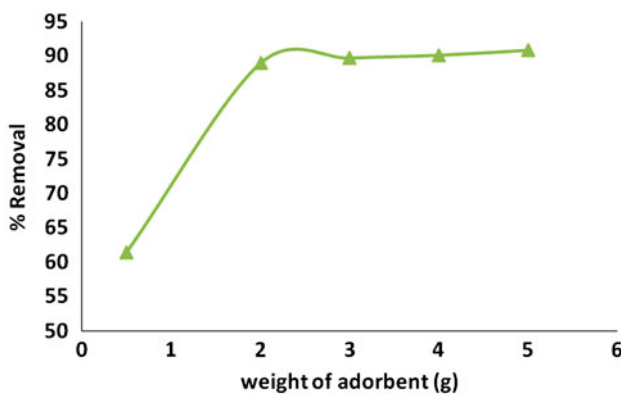


Fig. 7. Effect of initial weight of adsorbent on the removal efficiency% of Fe(III) ions using AC1 (Initial concentration of Fe(III): 30 ppm, pH=5, Contact time: 1 h).

### 3.5.1. Modeling of adsorption isotherm

The analysis of the isotherm data is important to develop an equation which accurately represents the results and could be used for design purposes. In order to investigate the adsorption isotherm, the adsorption data can be interpreted using several relationships which describe the distribution of Fe(III) molecules between the aqueous and solid phases. In order to investigate the adsorption isotherm, the experimental data of equilibrium isotherms were interpreted using four equilibrium models: the Freundlich, the Langmuir, the Tempkin, and the Dubinin–Radushkevich (D–R) isotherm equations. This modeling permits us to determine the maximal capacity of removal.

**3.5.1.1. Langmuir isotherm.** Langmuir's isotherm model suggests that the uptake occurs on homogeneous surface by monolayer sorption without interaction between adsorbed ions. The linear form of the Langmuir isotherm equation is represented by the following equation:

$$\frac{C_e}{q_e} = \frac{1}{Q^0 b} + \frac{1}{Q^0} C_e \quad (2)$$

where  $Q^0$  is the maximum Fe(III) ions uptake per unit mass of activated carbon (mg/g) related to adsorption capacity and  $b$  is Langmuir constant (L/mol) related to the energy of sorption. Therefore, a plot of  $C_e/q_e$  vs.  $C_e$  gives a straight line of slope  $1/Q^0$  and intercept  $1/(Q^0 b)$ . Table 2 shows that the experimental data were fitted by the linear form of Langmuir model,  $(C_e/q_e)$  vs.  $C_e$ . The values of  $Q^0$  and  $b$  were evaluated from the slope and intercept, respectively. These values of  $Q^0$  and  $b$  are listed in Table 1, with their uncertainty and their determination coefficients,  $R^2$ .

The results obtained from the Langmuir model for the removal of Fe(III) onto activated carbon are shown in Table 2.

**3.5.1.2. The Freundlich isotherm.** Freundlich isotherm describes the adsorption equation for non-ideal adsorption that involves heterogeneous adsorption. This empirical isotherm is expressed by the following equation:

$$q_e = K_F C_e^{1/n} \quad (3)$$

The equation is conveniently used in the linear form by taking the logarithm of both sides as:

$$\log q_e = \log K_F + \frac{1}{n} \log C_e \quad (4)$$

Freundlich constants,  $K_F$  and  $1/n$ , are related to adsorption capacity and intensity of adsorption, respectively. The values of  $n$  and  $K_F$  can be calculated from the slope and intercept of the plot of  $\log q_e$  vs.  $\log C_e$  derived from Eq. (4). The magnitude of the

Table 2  
Comparison of the coefficients isotherm parameters for Fe (III) adsorption onto AC1

Isotherm model	AC1
<i>Langmuir</i>	
$Q_m$ (mg g <sup>-1</sup> )	666
$K_a$ (L mg <sup>-1</sup> )	0.012
No. of parameter estimated	2
Data point available	4
$R^2$	0.8124
<i>Freundlich</i>	
$1/n$	0.7924
$K_F$ (mg g <sup>-1</sup> )	0.0229
No. of parameter estimated	2
Data point available	4
$R^2$	0.9696
<i>Tempkin</i>	
$B$ (mg g <sup>-1</sup> )	258.69
$\alpha$ (L mg <sup>-1</sup> )	0.0013
$b$ (kJ/mol)	9.58
No. of parameter estimated	2
Data point available	4
$R^2$	0.9718
<i>Dubinin–Radushkevich</i>	
$Q_m$ (mg g <sup>-1</sup> )	240.086
$v$	$2 \times 10^{-5}$
No. of parameter estimated	2
Data point available	4
$R^2$	0.9824

exponent  $1/n$  gives an indication of the favorability of adsorption.

The applicability of the Freundlich sorption isotherm was also analyzed, using the same set of experimental data, by plotting  $\log(q_e)$  vs.  $\log(C_e)$ . The data obtained from linear Freundlich isotherm plot for the adsorption of the Fe(III) onto activated carbon is presented in Table 1. The correlation coefficients reported in Table 2 showed strong positive evidence on the adsorption of Fe(III) onto activated carbon following the Freundlich isotherm. The applicability of linear forms of Freundlich model to activated carbon was proved by the high correlation coefficients  $R^2 > 0.96$ . This suggests that the Freundlich isotherm provides a good model for the sorption system. The  $1/n$  is lower than 1.0, indicating that Fe(III) is favorably adsorbed by activated carbon.

**3.5.1.3. The Tempkin isotherm.** Tempkin adsorption isotherm model was used to evaluate the adsorption potentials of the activated carbon for Fe(III). The derivation of the Tempkin isotherm assumes that the fall in the heat of sorption is linear rather than logarithmic, as implied in the Freundlich equation. The Tempkin isotherm is commonly been applied in the following form [26–28]:

$$q_e = \frac{RT}{b} \ln(AC_e) \quad (5)$$

The Tempkin isotherm Eq. (5) can be simplified to the following equation:

$$q_e = \beta \ln \alpha + \beta \ln C_e \quad (6)$$

where  $\beta = (RT)/b$ ,  $T$  is the absolute temperature in Kelvin, and  $R$  is the universal gas constant,  $8.314 \text{ J} (\text{molK})^{-1}$ . The constant  $b$  is related to the heat of adsorption [29,30]. The adsorption data were analyzed according to the linear form of the Tempkin isotherm Eq. (6).

Examination of the data shows that the Tempkin isotherm fitted the Fe(III) adsorption data for activated carbon well. The linear isotherm constants and coefficients of determination are presented in Table 2.

The heat of Fe(III) adsorption onto activated carbon was found to be  $9.58 \text{ kJ mol}^{-1}$

The correlation coefficients  $R^2$  obtained from Tempkin model were comparable to those obtained for Freundlich equation, which explains the applicability of Tempkin model to the adsorption of Fe(III) onto activated carbon.

#### 3.5.1.4. The Dubinin–Radushkevich (D–R) isotherm.

The D–R model was also applied to estimate the porosity apparent free energy and the characteristics of adsorption [31–33]. The D–R isotherm does not assume a homogeneous surface or constant sorption potential. The D–R model been applied in the following Eq. (7) and its linear form can be shown in Eq. (8):

$$q_e = q_m \exp(-K\varepsilon^2) \quad (7)$$

$$\ln q_e = \ln q_m - K\varepsilon^2 \quad (8)$$

where  $K$  is a constant related to the adsorption energy,  $Q_m$  is the theoretical saturation capacity, and  $\varepsilon$  the Polanyi potential calculated from Eq. (9).

$$\varepsilon = RT \ln \left( 1 + \frac{1}{C_e} \right) \quad (9)$$

The slope of the plot of  $\ln q_e$  vs.  $\varepsilon^2$  gives  $K$  ( $\text{mol}^2 (\text{kJ}^2)^{-1}$ ) and the intercept yields the adsorption capacity,  $Q_m$  ( $\text{mg g}^{-1}$ ). The calculated value of D–R parameters is given in Table 2. The saturation adsorption capacity  $Q_m$  obtained using D–R isotherm model for adsorption of Fe(III) onto activated carbon is  $240.086 \text{ mg g}^{-1}$ , which is close to the one obtained from Tempkin isotherm model ( $258.69 \text{ mg g}^{-1}$ ) (Table 2).

#### 3.6. Kinetic models applied to the adsorption of Fe(III) onto activated carbon

Kinetics of adsorption are one of the most important characteristics to be responsible for the efficiency of adsorption. The adsorbate can be transferred from the solution phase to the surface of the adsorbent in several steps and one or any combination of which can be the rate-controlling mechanism: (i) mass transfer across the external boundary layer film of liquid surrounding the outside of the particle; (ii) diffusion of the adsorbate molecules to an adsorption site by either a pore diffusion process through the liquid-filled pores or a solid surface diffusion mechanism; and (iii) adsorption (physical or chemical) at a site on the surface (internal or external), and this step is often assumed to be extremely rapid.

The overall adsorption can occur through one or more steps. In order to investigate the mechanism of process and potential rate-controlling steps, the kinetics of Fe(III) adsorption onto activated carbon were analyzed using pseudo-first-order [34], pseudo-second-order [35], Elovich [36], and fractional power

[37,38] kinetic models. The conformity between experimental data and the model-predicted values was expressed by the correlation coefficients ( $R^2$ , values close or equal to 1). The relatively higher value is the more applicable model to the kinetics of Fe(III) adsorption onto activated carbon.

### 3.6.1. Pseudo-first-order equation

The adsorption kinetic data were described by the Lagergren pseudo-first-order model [34], which is the earliest known equation describing the adsorption rate based on the adsorption capacity. The linear form equation is generally expressed as follows:

$$\log(q_e - q_t) = \log q_e - \frac{K_1}{2.303} t \quad (10)$$

In order to obtain the rate constants, the values of  $\log(q_e - q_t)$  were linearly correlated with  $t$  by plot of

$\log(q_e - q_t)$  vs.  $t$  to give a linear relationship from which  $K_1$  and predicted  $q_e$  can be determined from the slope and intercept of the plot, respectively.

The variation in rate should be proportional to the first power of concentration for strict surface adsorption. However, the relationship between initial solute concentration and rate of adsorption will not be linear when pore diffusion limits the adsorption process. The experimental  $q_e$  values do not agree with the calculated ones obtained from the linear plots, and the correlation coefficient  $R^2$  are relatively low for most adsorption data (Table 2). This shows that the reaction mechanism of adsorption of Fe(III) is not a first-order reaction.

### 3.6.2. Pseudo-second-order equation

The adsorption kinetic may be described by the pseudo-second-order model. The linear equation is generally given as follows:

Table 3  
Kinetic parameters for the adsorption of Fe(III) onto activated carbon

Kinetics models	AC1	AC2	Raw rice straw
<i>Zero-order kinetics</i>			
$Q_e$ (mg g <sup>-1</sup> )	28.205	23.884	13.604
$K$ (mg g <sup>-1</sup> s <sup>-1</sup> )	-0.3253	-0.1104	-0.2046
$R^2$	0.7268	0.7525	0.6154
<i>First-order kinetics</i>			
$K_1$ (min)	-0.0085	-0.0035	-0.0118
$q_1$ (mg/g)	3.2951	3.4759	2.4363
$R_1^2$	0.5947	0.7525	0.4936
<i>Pseudo-first-order kinetics</i>			
$K_1$ (min)	0.0374	0.0194	0.0241
$q_1$ (mg/g)	51.935	18.688	21.538
$R_1^2$	0.945	0.9588	0.7724
<i>Second-order kinetics</i>			
$K_2$ (g/mg min)	-0.0003	-9E-5	-0.0009
$Q_2$ (mg/g)	25.45	32.362	9.234
$R_2^2$	0.468	0.7387	0.3284
<i>Pseudo-second-order kinetics</i>			
$K_2$ (g/mg min)	0.0008	0.00049	0.00089
$q_2$ (mg/g)	68.966	45.045	41.322
$R_2^2$	0.9859	0.9989	0.936
<i>Elovich</i>			
$\alpha$ (mg g <sup>-1</sup> min <sup>-1</sup> )	14.456	5.0721	9.6648
$\beta$ (g mg <sup>-1</sup> )	0.043804	11.546	0.035606
$R_E^2$	0.932	0.95	0.891
<i>Fractional power</i>			
$K$ mgg <sup>-1</sup>	10.03315	23.4858	2.47
$v$	0.4016	0.1382	0.4
$R^2$	0.8553	0.9517	0.8344

$$\frac{t}{q_t} = \frac{1}{K_2} \frac{1}{q_e^2} + \frac{1}{q_e} t \quad (11)$$

If the second-order kinetics is applicable, then the plot of  $t/q_t$  vs.  $t$  should show a linear relationship. Values of  $K_2$  and equilibrium adsorption capacity  $q_e$  were calculated from the intercept and slope of the plots of  $t/q_t$  vs.  $t$ . The linear plots of  $t/q_t$  vs.  $t$  show good agreement between experimental and calculated  $q_e$  values (Table 3). The correlation coefficients for the second-order kinetic model are greater than 0.98, which led to the belief that the pseudo-second-order kinetic model provided good correlation for the adsorption of Fe(III) onto activated carbon and raw rice husk.

### 3.6.3. Elovich equation

The Elovich equation is generally expressed as follows:

$$q_t = \beta \ln(\alpha\beta) + \beta \ln t \quad (12)$$

If Fe(III) adsorption by activated carbon fits the Elovich model, a plot of  $q_t$  vs.  $\ln(t)$  should yield a linear relationship with a slope of  $\beta$  and an intercept of  $\beta \ln(\alpha\beta)$ . Thus, the constants can be obtained from the slope and the intercept of the straight line (Table 3). High correlation coefficient values ( $>0.997$ ) for the pseudo-second-order kinetic model in all conditions revealed that the Fe(III) uptake process followed the pseudo-second-order rate expression.

The calculated  $q_e$  values agree very well with the experimental data in the case of pseudo-second-order kinetics for activated carbon produced by chemical activation (first method (AC1)), activated carbon produced by chemical activation (second method (AC2)), and raw rice straw husk. According to the pseudo-second-order model, the adsorption rates become very fast and the equilibrium times are short, which are confirmed by the experimental results.

## 4. Conclusion

The Egyptian rice straw as a potential feedstock was used for the preparation of activated carbon. Chemical activation of this precursor using two different methods was adopted. The produced activated carbons from the two methods (AC1 and AC2) were used as potential adsorbents for the removal of Fe(III) from aqueous solution.

Based on the experimental results, the optimum contact time is 60 min and adsorbent dosage is 3 g/L. The adsorption of Fe(III) was found to be dependent on the pH of the solution. The optimal Fe(III) removal

efficiency occurs at pH 5. The Freundlich adsorption isotherm model describes the adsorption behavior with good correlation coefficient. The  $1/n$  value from Freundlich model is lower than 1.0, indicating that Fe(III) is favorably adsorbed by the activated carbon. The metal ion adsorption obeyed the pseudo-second-order model based on the experimental and calculated  $q_e$  values.

## References

- [1] J.S. Mattson, H.B. Mark, Activated Carbon, Dekker, New York, NY, 1971.
- [2] F.S. Baker, C.E. Miller, A.J. Repic, E.D. Tolles, Activated carbon, Kirk-Othmer Encyclopedia of Chemical Technology 4 (1992) 1015–1037.
- [3] A.A. El-Hendawy, Influence of HNO<sub>3</sub> oxidation on the structured and adsorptive properties of corncob activated carbon, Carbon 41 (2003) 713–722.
- [4] D. Cuhadaroglu, O.A. Uygun, Production and characterization of activated carbon from a bituminous coal by chemical activation, Afr. J. Biotechnol. 7(20) (2008) 3703–3710.
- [5] L. Khezamiet, A. Chetouani, B. Taouk, R. Capart, Production and characterization of activated carbon from wood components in powder: Cellulose, lignin, xylan, Powder Technol. 157 (2005) 48–56.
- [6] C. Srinivasakannan, M.Z. Abu Bakar, Production of activated carbon from rubber wood sawdust, Biomass Bioenergy 27(1) (2004) 89–96.
- [7] N. Pasadakis, G. Romanos, V. Perdikatsis, A.E. Foscolos, The production of activated carbons using Greek lignites by physical and chemical activation methods: A Comparative Study, Energy Sources 33(8) (2011) 713–723.
- [8] M.Z. Hussein, R.S.H. Tarmizi, Z. Zainal, R. Ibrahim, M. Badri, Preparation and characterization of activated carbons from oil palm coconut shells, Carbon 34 (1996) 1447–1449.
- [9] M.K. Gratuito, B.T. Panyathanmaporn, R.A. Chumnanklang, N. Sirinuntawittaya, A. Dutta, Production of activated carbon from coconut shell: Optimization using response surface methodology, Bioresour. Technol. 99 (2008) 4887–4895.
- [10] Z. Al-Qodah, R. Shawabkah, Production and characterization of granular activated carbon from activated sludge, Brazil. J. Chem. Eng. 26 (2009) 127–136.
- [11] J.W. Kim, M.H. Sohn, D.S. Kim, S.M. Sohn, Y.S. Kwon, Production of granular activated carbon from waste walnut shell and its adsorption characteristics for Cu(2+) ion, J Hazard Mater. 85(3) (2001) 301–315.
- [12] N. Buasri, C. Chaiyut, C. Nakweang, Preparing Activated Carbon from Palm Shell for Biodiesel Fuel Production, Chiang Mai J. Sci. 38(4) (2011) 572–578.
- [13] R.R. Bansode, J.N. Lasso, W.E. Marshall, R.M. Rao, R.J. Portier, Pecan shell-based granular activated carbon for treatment of chemical oxygen demand (COD) in municipal wastewater, Bioresour. Technol. 94 (2004) 129–135.
- [14] S.A. Dastgheib, D.A. Rockstraw, Pecan shell activated carbon: Synthesis, characterization, and application for the removal of copper from aqueous solution, Carbon 39 (2001) 1849–1855.
- [15] Y.A.S. Alhamed, Activated Carbon from Dates' Stone by ZnCl<sub>2</sub> activation, JKAU: Eng. Sci. 17 (2006) 75–100.
- [16] Bhatti, K. Qureshi, R.A. Kazi, A. Ansari, Preparation and characterisation of chemically activated almond shells by optimization of adsorption parameters for removal of chromium vi from aqueous solutions, World Academy of Sci. Eng. Technol. 34 (2007) 199–204.
- [17] E.F. Jaguaribe, L.L. Medeiros, M.C.S. Barreto, L.P. Araujo, The performance of activated carbons from sugarcane bagasse, babassu, and coconut shells in removing residual chlorine, Brazil. J. Chem. Eng. 22 (2005) 41–47.

- [18] M. El Zayat, E. Smith, Removal of heavy metals by using activated carbon produced from cotton stalks, *Can. J. Environ. Construction Civil Eng.* 1(4) (2010) 71–79.
- [19] P. Chiravoot, A. Duangdao, A. Duangduen, S. Viboon, Physicochemical properties of carbons prepared from physic nut waste by phosphoric acid and potassium hydroxide activations, *Mater. Sci. Forum* 561–565 (2007) 1719–1722.
- [20] P. Gao, Z.H. Liu, G. Xue, B. Han, M.H. Zhou, Preparation and characterization of activated carbon produced from rice straw by  $(\text{NH}_4)_2\text{HPO}_4$  activation, *Bioresour. Technol.* 102(3) (2011) 3645–3648.
- [21] N. Yahaya, E.M. Pakir, M.F. Latiff, M.I. Abustan, M.A. Ahmad, Effect of preparation conditions of activated carbon prepared from rice husk by  $\text{ZnCl}_2$  activation for removal of Cu (II) from aqueous solution, *Int. J. Eng. Technol. IJET-IJENS* 10(6) (2010) 27–31.
- [22] N. Yeddou, A. Bensmaili, Equilibrium and kinetic modeling of iron adsorption by egg shells in a batch system: effect of temperature, *Desalination* 206 (2007) 127–134.
- [23] G. Karthikeyan, A.N. Muthulakshmi, K. Anbalagan, Adsorption studies of iron (III) on chitin, *J. Chem. Sci.* 117 (2005) 663–672.
- [24] Z.A. Al-Anber, M.A.S. Al-Anber, Thermodynamics and kinetic studies of iron(III) adsorption by Olive Cake in a batch system, *J. Mex. Chem. Soc.* 52(2) (2008) 108–115.
- [25] K.N. Ghimire, K. Inoue, K. Ohto, Heavy metal removal from contaminated scallop waste for feed and fertilizer application, *Bioresour. Technol.* 99 (2008) 2436–2441.
- [26] C. Aharoni, D.L. Sparks, Kinetics of soil chemical reactions—a theoretical treatment, In: D.L. Sparks, D.L. Suarez (Eds.), *Rate of Soil Chemical Processes*, Soil Science Society of America, Madison, WI, pp. 1–18, 1991.
- [27] C. Aharoni, M. Ungarish, Kinetics of activated chemisorption. Part 2. Theoretical models, *J. Chem. Soc., Faraday Trans.* 73 (1977) 456–464.
- [28] X.S. Wang, Y. Qin, Equilibrium sorption isotherms for of  $\text{Cu}^{2+}$  on rice bran, *Process Biochem.* 40 (2005) 677–680.
- [29] G. Akkaya, A. Ozer, Adsorption of acid red 274 (AR 274) on *Dicranella varia*: Determination of equilibrium and kinetic model parameters, *Process Biochem.* 40(11) (2005) 3559–3568.
- [30] C.I. Pearce, J.R. Lloyd, J.T. Guthrie, The removal of color from textile wastewater using whole bacterial cells: A review, *Dyes Pigm.* 58 (2003) 179–196.
- [31] M.M. Dubinin, Modern state of the theory of volume filling of micropore adsorbents during adsorption of gases and steams on carbon adsorbents, *Zhurnal Fizicheskoi Khimii [Russ. J. Phys. Chem. A]* 39 (1965) 1305–1317.
- [32] M.M. Dubinin, The potential theory of adsorption of gases and vapors for adsorbents with energetically non-uniform surface, *Chem. Rev.* 60 (1960) 235–266.
- [33] L.V. Radushkevich, Potential theory of sorption and structure of carbons, *Zhurnal Fizicheskoi Khimii [Russ. J. Phys. Chem. A]* 23 (1949) 1410–1420.
- [34] S. Lagergren, Zur theorie der sogenannten adsorption geloster stoffe, *Svenska Vetenskapsakademiens. Handlingar* 24(4) (1898) 1–39.
- [35] Y.S. Ho, G. McKay, D.A.J. Wase, C.F. Foster, Study of the sorption of di-valent metal ions on to peat, *Adsorpt. Sci. Technol.* 18 (2000) 639–650.
- [36] S.H. Chien, W.R. Clayton, Application of Elovich equation to the kinetics of phosphate release and sorption on soils, *Soil Sci. Soc. Am. J.* 44 (1980) 265–268.
- [37] W.J. Weber, J.C. Morris, Kinetics of adsorption on carbon from solution, *J. Sanitary Eng. Div. Am. Soc. Civil Eng.* 89 (1963) 31–59.
- [38] K. Srinivasan, N. Balasubramanian, T.V. Ramakrishan, Studies on chromium removal by rice husk carbon, *Indian J. Environ. Health* 30 (1988) 376–387.